Junichi Inamoto[1]
Yoshiaki Matsuo[1], Katsumi Maeda[2], Masashi Ishikawa[3], Satoshi Uchida[4], Takuya Masuyama[5], Kaoru Tsukamoto[5], Yuta Sato[6]
[1]Univ. Hyogo, Himeji, Japan, [2]NEC corp., Tsukuba, Japan, [3]Kansai Univ., Suita, Japan, [4]AIST, Ikeda, Japan, [5]Nippon Graphite, Otsu, Japan, [6]AIST, Tsukuba, Japan

j.inamoto@eng.u-hyogo.ac.jp

Scanning Tunneling Microscopic Analysis of Graphene-Like Graphite Synthesized from Highly Oriented Pyrolytic Graphite

Introduction

Recent advancement of lithium-ion batteries (LIBs) has realized practical use of electric vehicles (EVs) as well as portable devices. As a negative electrode material of LIBs, graphite has been widely used for over two decades. Although graphite shows good reversibility and cycleability, it is almost impossible to further extend its capacity. Moreover, graphite suffers from poor rate capability, which is a serious disadvantage for the use of EVs. Therefore, alternative anode materials with large capacity and good rate capability has been expected. One of the most promising candidates is graphene. Graphene has much larger capacity and better rate capability than graphite. However, graphene suffers from poor reversibility and cycleability, and it is mainly because of its large specific surface area. In short, graphite and graphene have the opposite advantages and disadvantages. If the material with the both advantages of these materials, it should have ideal properties as a negative electrode material. In this term, we have recently proposed a new carbon-based material named graphene-like graphite (GLG), which has both properties of graphite and graphene [1]. GLG is composed of stacked graphene layers with some oxygen-containing groups. The interlayer distance of GLG is a little larger than that of graphite. GLG has much less specific surface area than graphene, and it contributed to suppressed irreversible capacity like graphite. In addition, capacity and rate capability of GLG are comparable to those of graphene. However, the structural characteristics of GLG has been not completely understood yet. In this study, we focused on analysis of the structure of GLG with scanning tunneling microscopy (STM). For STM measurement, a macroscopic sample with flat surface is required. Therefore, we synthesized GLG mono-sheets from highly oriented pyrolytic graphite (HOPG), and their structure at the surface region was investigated.

Experimental

Highly oriented pyrolytic graphite (HOPG, ZYH-grade) was oxidized with fuming HNO_3 aq. and $KClO_3$ at 60°C based on Brodie's method to obtain graphite oxide (GO). The resulting GO was reduced at 700°C under vacuum to obtain GLG mono-sheets. X-ray diffraction patterns of HOPG, GO and GLG indicated that GO had no residue of HOPG, and interlayer distance of GLG was similar to that of HOPG. The GLG mono-sheets were analyzed with scanning tunneling microscopy with 0.1 V of bias voltage. In addition to the STM measurement, density functional theory (DFT) calculations of HOPG and GLG were conducted for optimization of the structures using slab model supercells and simulation of STM images to interpret the experimental STM images. To simulate STM images, partial charge density around 0.1 V above the Fermi level was calculated, and the densities above the top layers were projected as 2D images. As well as the normal GLG mono-sheet, a GLG mono-sheet treated with hydrogen gas, which we have found effective to decrease mean-discharge potential and increase the capacity [2], was also analyzed using STM together with the simulation.

Results and Discussion

Figure 1 shows STM images of HOPG, GLG and H_2-treated GLG (hereafter GLG-H). HOPG (Fig. 1 (a)) showed well-ordered triangular bright points. This unique pattern was caused by C atoms at β site on the top layer [3], and it indicated that the HOPG was well-crystallized graphite with AB-stacking graphene layers. On

the other hand, GLG (Fig. 1 (b)) showed a considerably distorted and disordered image. It indicated that oxygen-containing group inside distorted the graphene layer. In addition, 6-membered ring was observed at the region designated by red dotted line. After the H_2 gas treatment (Fig.1 (c)), GLG-H recovered the well-ordered triangular points, which was similar to HOPG. In order to interpret these experimental images, simulation of STM images was conducted. Simulated image of HOPG (Fig. 2 (a)) was good agreement with the experimental image. We also confirmed that this calculation condition was suitable for the simulation. To simulate STM image of GLG, ether O atoms were introduced into the second layer from the top. Existence of ether groups expanded interlayer spacing after structural relaxation, resulting in 6-membered rings in the simulated image of GLG (Fig. 2 (b)), which corresponded to the experimental image. From the results, it was suggested that ether O atoms existed in the bulk of GLG and it caused expansion of the interlayer spacing. In order to simulate STM image of GLG-H, the one O atom introduced in the model supercell of GLG was replaced with two H atoms, and the DFT calculation was conducted. Unlike the model of GLG, introduction of H-containing groups inside the bulk did not expanded the interlayer spacing. As a result, the triangular bright points were observed (Fig. 2 (c)), which was good agreement with the experimental result. From the results, H_2 gas treatment removed ether O atoms inside the bulk of GLG, and it reduced the distortion of graphene layers. Although an oxygen atom was not observed at the top layer, the 6-membered ring observed for GLG and re-appearance of triangular points observed for GLG-H indicated that the existence of oxygen atoms inside GLG and their reduction after H_2 gas treatment. Since the treatment decreased the distortion of graphene layers and the structure became similar to graphite, it possibly lowered mean-discharge potential of GLG-H, resulting in larger accessible capacity at lower potential.

References

[1] Q. Cheng, Y. Okamoto, M. Tsuji, N. Tamura, S. Maruyama, and Y. Matsuo, *Sci. Rep.*, **7** (2017) 14782.

[2] Y. Matsuo, J. Taninaka, K. Hashiguchi, T. Sasaki, Q. Cheng, Y. Okamoto, and N. Tamura, *J. Power Sources*, **396** (2018) 134.

[3] D. Tománek, S. G. Louie, H. J. Mamin, D. W. Abraham, R. E. Thomson, E. Ganz, and J. Clarke, *Phys. Rev B*, **35** (1987) 7790.

Figures

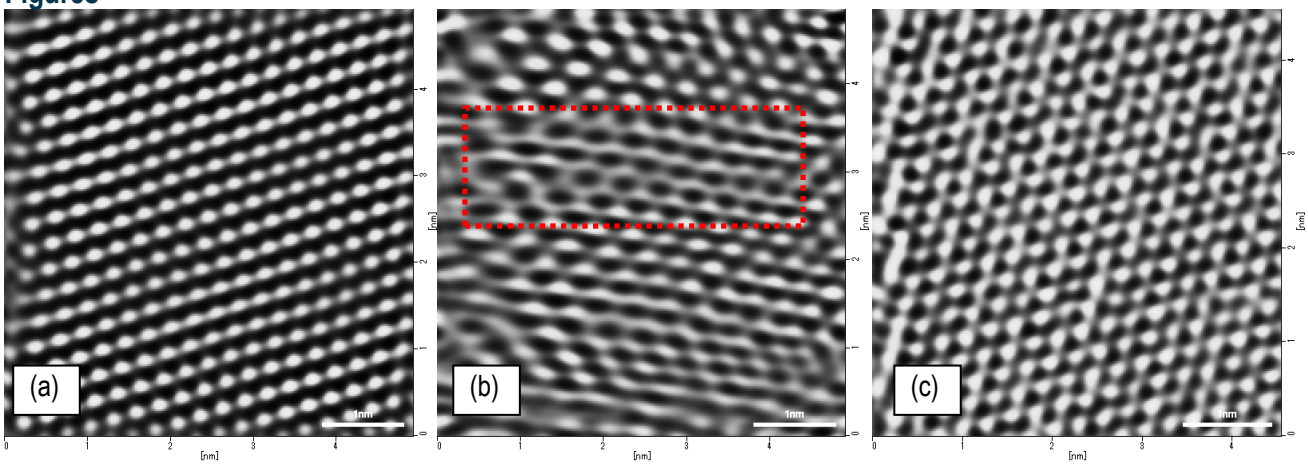

Figure 1: Scanning tunneling microscopic images of HOPG (a), GLG (b) and GLG-H (c).

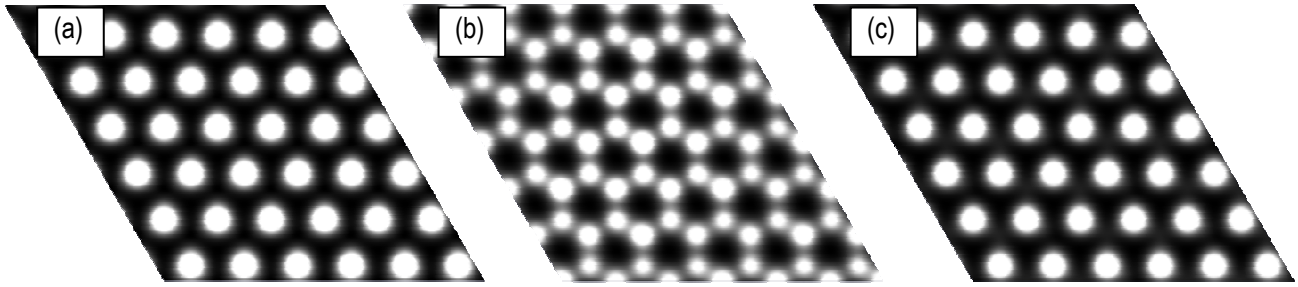

Figure 2: Simulated STM images of HOPG (a), GLG (b) and GLG-H (c).